HHS Public Access

Author manuscript

J Biochem Mol Toxicol. Author manuscript; available in PMC 2015 June 14.

Published in final edited form as:

J Biochem Mol Toxicol. 2009 ; 23(3): 172–184. doi:10.1002/jbt.20275.

Upregulation of Gamma-2 Laminin-332 in the Mouse Ear Vesicant Wound Model

Yoke-Chen Chang[1], **Carol L. K. Sabourin**[2], **Shou-En Lu**[3], **Takako Sasaki**[4], **Kathy K. H. Svoboda**[5], **Marion K. Gordon**[1], **David J. Riley**[6], **Robert P. Casillas**[2], and **Donald R. Gerecke**[1]

[1]Department of Pharmacology & Toxicology, Ernest Mario School of Pharmacy, Rutgers University, EOHSI, 170 Frelinghuysen Road, Piscataway, NJ 08854, USA

[2]Battelle Memorial Institute, 505 King Avenue, Columbus, OH 43201-2693, USA

[3]Department of Biostatistics, UMDNJ School of Public Health, 683 Hoes Lane West, Piscataway, NJ 08854, USA

[4]Department of Molecular Biology & Biochemistry, Oregon Health & Science University, Portland, OR 97239, USA

[5]Biomedical Sciences, Texas A&M Health Science Center, Baylor College of Dentistry, Dallas, TX 75246, USA

[6]Department of Medicine, UMDNJ–Robert Wood Johnson Medical School, 675 Hoes Lane West, Piscataway, NJ 08854, USA

Abstract

Epithelial cell migration during wound healing is regulated in part by enzymatic processing of laminin-332 (formerly LN-5), a heterodimer formed from α, β, and γ polypeptide chains. Under static conditions, laminin-332 is secreted into the extracellular matrix as a proform and has two chains processed to smaller forms, allowing it to anchor epithelial cells to the basement membrane of the dermis. During incisional wounding, laminin γ2 chains in particular are processed to smaller sizes and function to promote epithelial sheet migration over the wound bed. The present study examines whether this same function occurs following chemical injury. The mouse ear vesicant model (MEVM) was used to follow the pathology in the ear and test whether processed laminin-332 enhances epithelial cell migration. Skin biopsies of sulfur mustard (SM) exposed ears for several time points were analyzed by histology, immunohistochemistry, real-time PCR, and Western blot analysis. SM exposure greatly increased mRNA levels for laminin-γ2 in comparison to the other two chains. Protein production of laminin-γ2 was upregulated, and there was an increase in the processed forms. Protein production was in excess of the amount required to form heterotrimeric laminin-332 and was associated with the migrating epithelial sheet, suggesting a potential role in wound healing for monomeric laminin-γ2.

Correspondence to: Donald R. Gerecke, gerecke@eohsi.rutgers.edu..

Keywords

Sulfur mustard; Laminin; Wound, Mouse ear vesicant model; Vesicant

INTRODUCTION

Epithelial cell migration during wound repair in skin is critical to the healing process. It requires the cells to alter their phenotype from a normal, stationary state to one that is migratory. Proteins that normally anchor the keratinocytes to maintain skin integrity are required to become detached so the cells can move. One of these anchoring proteins, laminin-332 (formerly laminin-5), is a component of skin basement membrane and functions to help maintain skin integrity by directly connecting the basal keratinocytes of the epithelium to collagen VII in the dermis below [1-3]. To function as an "anchoring filament," the laminin-332 attaches the carboxyl terminal end of the α3 chain to α6β4 integrin, a protein localized in the electron dense hemidesmosomes that are embedded in the cell membrane of the basal keratinocytes [4,5]. The amino terminal end of the laminin β3 polypeptide chain is in turn attached to collagen VII [4,6,7]. Laminin-332 protein is actually composed of three separate polypeptides connected by disulfide bonds (Figure 1). The three chains (laminin α3, β3, and γ2) together form an alpha helix (shown schematically in Figure 1). All three chains are sensitive to proteolytic cleavage resulting in a variety of sizes (cleavage sites indicated by arrows in Figure 1) [8,9]. This proteolytic processing is required for the keratinocytes to switch from an adhesive to a migratory state [10]. Enzymatic processing of laminin-332 also occurs in epithelial-derived carcinoma cells when they switch from a stationary to a migratory phenotype [11,12]. The proteolytic processing of the laminin α3 and laminin γ2 chains in particular has been implicated in promoting the cell migration activity of laminin-332. Potential processing forms for laminin γ2 and their sizes are shown in Figure 2. However, all of the potential processed forms have not been identified in vivo [13-15]. The increased keratinocyte migration attributed to laminin γ2 processing from a proform (Figure 2; Np-LN5; ~150 kDa) to a smaller, 105 kDa, (Figure 2 Pr-LN5) size has also been demonstrated using recombinant technology [16]. The results from that study indicated that the release of domains g2 LEa1-3 + L4 as a single unit from the laminin γ2 chain promotes cell adhesion via the syndecan-1 surface receptor (Figure 2; γ2pf). Still other researchers suggest that a processed 80 kDa, containing domains g2 LEa2-3 + L4 + LEb1-3 (Figure 2; γ2sa) may be involved in keratinocyte migration [11]. Finally, although it is unclear whether the laminin γ2 chain by itself can promote nontransformed keratinocyte migration in vivo, monomeric laminin γ2 has been demonstrated to enhance migration in invasive carcinoma cells [17]. There is extensive literature regarding the role of laminin-332 in carcinoma cell migration, showing the monomeric form is preferentially expressed in the leading edge of nonchemically induced wounds [18,19]. There are few reports regarding the influence of laminin-332 on keratinocyte migration over chemical-induced wounds and burns.

We previously used the mouse ear vesicant model (MEVM) to study skin injury [20]. In the present study, mouse skin was exposed to a high level (0.08 mg) of sulfur mustard (SM) and samples were collected 6, 12, 24, 72, and 168 h postexposure. The expression patterns of the

various laminin-332 polypeptide chains were examined by immunohistochemistry and compared to two intermediate filament proteins, the general basic keratin type II and keratin 5. Furthermore, the possibility that the laminin γ2 chain protein is expressed as a monomer in the MEVM was investigated, and evidence is presented to show that that this chain is preferentially expressed by migrating keratinocytes and not in the hyperproliferating cells behind the leading edge of an epithelial sheet moving across a wound bed.

MATERIALS AND METHODS

RNA Isolation and Reverse Transcription

Total RNA was isolated the frozen ear punch biopsies using TRIzol reagent, according to the manufacture's instructions (Invitrogen Corporation, Carlsbad, CA). Eppendorf phase lock gel (Brinkmann Instruments, Westbury, NY), a product that eliminates interface-protein contamination during phenol extraction, was added during centrifugation. The RNA pellet was dissolved in RNA storage solution (Ambion, Austin, TX), and RNA was quantitated spectrophometerically based on absorbance at 260 nm. Total RNA (1 μg) was reverse-transcribed into cDNA using a first-strand synthesis system (Invitrogen) for reverse transcriptase-polymerase chain reaction (RT-PCR). A minus reserves transcriptase reaction was included as a control.

Real-Time Polymerase Chain Reaction

Primer and probe sets for Ln-α3 (X84013), Ln-β3 (NM_008484), Ln-γ2 (U43327), and hypoxanthine guanine phosphoribosyl transferase (NM_013556) (used as an endogenous control) were designed by the TaqMan Assay-By-Design service (Applied Biosystems, Foster City, CA; accession numbers for primer designs are shown in parentheses). The mRNA levels were measured from samples taken at 24, 72, and 168 h by real-time RT-PCR. The primer pairs were generated from GenBank sequences. Assays were performed in duplicate and averaged. No template controls were negative for amplification. Data were expressed as fold change relative to dichloromethane (CH_2Cl_2) control, and the fold changes in RNA between the SM-treated and numbers and primer pairs for RT-PCR are as follows.

Western Blot Analyses

The extraction of tissues samples for Western-blot was performed as previously described [21].

Statistics

The fold change over time was log-transformed and assessed with the weighted one-way analysis of variance (ANOVA). The weights for the observations in each group (time point) were assigned as the reciprocals of the error variances separately calculated at each time point. Statistical analyses were conducted using the PROC GLM procedure with the weight option of SAS version 9.1 for the personal computer (SAS Institute Inc, Cary, NC). A p value of <0.05 was defined as significant. Bonferonni correction was applied for multiple testing, as appropriate.

Immunohistochemistry and Immunofluorescence

Immunohistochemistry—Immunohistochemical staining for laminin α3, β3, and γ2 and keratin 5 were carried out with a Vectastain Elite ABC kit (Vector Laboratories, Inc., Burlingame, CA). Paraffin-embedded tissue sections were deparaffinized and rehydrated, and endogenous peroxidase activity was blocked by incubating the sections in 3% hydrogen peroxide. The sections were treated with 5% normal goat serum or CAS-BLOCK (Zymed Laboratories, Invitrogen Immunodection, San Francisco, CA) to block nonspecific binding and incubated overnight at 4°C (for a goat, antikeratin type II (ab8572, Abcam); rabbit, laminin α3, β3 and γ2; diluted 1:500 in PBS/0.05% Tween-20/1.5% NGS) or 1 h room temperature (a rabbit, antikeratin-5, ab24647, abcam, MA; diluted 1:1000 in PBS/0.05% Tween-20/1.5% NGS) with primary antibodies. The chain-specific laminin antibodies were rabbit anti-human polyclonal antiserum. (gifts from Dr. Takako Sasaki [22] (for laminin α3(ab1110+; α3IIIa), β3 (ab1111+, β3VI/V), and γ2(ab1097+, γ2 LE4–6, ab1084+ γ2 L4m)]. The sections incubated for 30 min at room temperature with botinylated goat, anti-rabbit secondary antibody (diluted 1:200 in PBS/0.05% Tween-20/1.5% NGS), followed by avidin–biotin–horseradish peroxidase complex (diluted 1:50) for 30 min at room temperature. For color development, 3.3′-diaminobenzidine tetrahydrochloride (Sigma, St. Louis, MO) was added for 2–10 min, and the slides washed in water to stop reaction. The slides were counterstained with hematoxylin, dehydrated and mounted in Permount (Fisher, Fair Lawn, NJ), and cover slips were applied. Secondary only controlled were carried out with normal goat serum.

Immunofluorescence and Confocal—Paraffin-embedded tissue sections were deparaffinized and rehydrated. The sections were blocked with 5%–10% normal donkey serum. Double immunofluorescent staining was carried out. Primary and secondary antibodies used were as follows: A goat antilaminin γ2 (sc-7652 (C-20), Santa Cruz Biotechnology, Inc., Santa Cruz, CA: a goat antikeratin II (ab8572; Abcam, Cambridge, MA; donkey anti-goat Alexa Fluor 568 and Alexa Fluor 488 (Invitrogen), rabbit antikeratin 5 (Abcam), and Cy3 (Jackson ImmunoResearch Lab. Inc., PA). The sections were applied with 10 μM DRAQ5 (1,5-bis[{2-(dimethylamino]-4,8-dihydroxyanthracene-9,10-dione], AXXORA, San Diego, CA) for 30 min in dark for nuclei staining. The sections were mounted in ProLong gold antifade reagent (Invitrogen/Molecular Probes, Eugene, OR), and cover slips were applied to cure overnight. The confocal images were collected with the Leica TCS SP2 spectral confocal microscope equipped with a tunable argon laser, a 561-nm diode laser, and two HeNe lasers (594 and 633 nm).

RESULTS

Edema, Inflammation, and Necrosis Progress over Time After Sulfur Mustard Exposure in the Mouse Ear Vesicant Model

Previous studies using the MEVM followed injury progression primarily in the first 24 h [20]. However, further experience using the MEVM indicates it produces more severe inflammation and pathological damage than incisional wound healing models as evidenced by progressive structural changes of the skin continuing even days after the initial exposure. This vesicant-induced wound progression was followed for up to 1 week after exposure.

Hematoxylin and eosin staining of mouse ears treated with SM confirmed earlier observations that there is inflammatory cell infiltration and pronounced edema within the first 24 h post-SM exposure of the treated ears compared to the untreated, naive samples (Figure 3) [23,24]. This is evident by significant swelling of the tissue as reflected by the increased distances between the ventral (anterior surface) and dorsal (posterior surface) sides of the ear and by an abundance of clear areas in the dermis (Figures 3a and 3b; note that these panels are identical magnifications). Edema increases beyond 24 h and is accompanied by significant neutrophil and monocyte infiltration, which is observed 72 h postexposure (Figure 3c; inflammatory cell nuclei stained purple). A pronounced inflammatory response commenced within 24 h and continually progressed throughout the study. Necrosis commonly occurs on the treated, ventral side by 72 h postexposure (Figure 3c, indicated by arrows). The wound area continues to expand, eventually including the dorsal, untreated side. The dorsal side temporally lags slightly behind the ventral side in severity of tissue damage. However, even on the untreated side, necrosis often becomes evident by 168 h postexposure (Figure 3d, necrotic areas indicated by arrows).

Normal, Untreated Tissue Has Moderate Expression of Laminin-332, Keratin Type II, and Keratin 5

To examine the expression of laminin-332 protein in the SM-exposed skin, five independent epitopes (indicated by arrows in Figure 1) were examined in a time-course study using serial tissue sections. Immunohistochemistry was performed for both SM-treated and solvent alone ($CHCl_2$) mouse ears. There appeared to be modest expression of all the laminin-332 polypeptide chains in the untreated ears (Figures 4c, 4d, and 4f–4h), and the expression was not confined to the dermal–epidermal junction. All three polypeptide chains of laminin-332 were observed to have uniform expression in all the layers of the epithelial cells in both the ventral anterior and dorsal posterior surfaces of the mouse ear skin. All three chains also lined the sebaceous glands of the dermis. The laminin β3 antibody (Figure 4d) did not stain intensively, suggesting that the epitope may be partially masked when laminin β3 is in the context of the laminin-332 anchoring filaments (in that situation, laminin β3 covalently interacts with collagen VII and may interfere with the antigen recognition site for the antibody). There was moderate expression of keratin type II and keratin 5 in control tissue sections (Figures 4b and 4e).

Increased Expression of Laminin-332, Keratin Type II, and Keratin 5 Occurs 24 h after SM Treatment

In 24 h post-SM-treated samples, the laminin α3, β3, and γ2 distribution overlapped with the epithelial layer for both the treated and untreated sides (Figures 5c, 5d, and 5f–5h). Their distributions were indistinguishable from the immunohistochemical staining pattern for the 24-h posttreated keratin type II and keratin 5 (Figures 5b and 5e); however, the signals were stronger when compared to the untreated control (Figure 4), suggesting either there was more corresponding protein present in the SM-treated ears, or that the epitopes were more accessible to the antibodies after SM treatment.

Wound Healing and Apoptosis Progress from 3 to 7 Days Postexposure

At 72 h post-SM-treatment, the laminin α3 and laminin β3 had a similar distribution to that of the keratinocyte markers keratin type II and keratin 5 (Figures 6b–6e). The immunohistochemical staining for laminin β3 was diffuse and faint in appearance and was either masked or not abundant. The epitopes for laminin γ2 were indistinguishable from keratin type II and keratin 5 (Figures 6b and 6e–6h). The untreated, dorsal side in the 72-h posttreated samples appeared to have hyperplasia; therefore, the sections were examined at higher magnification and showed intense staining in the epithelial cells for all the samples. These results are presented in Figure 7. Immunohistochemistry on tissue sections 168 h post-SM-exposure indicates that the epithelial cells have repopulated and covered the wound bed and express both keratin 5 and laminin γ2, although many cells have pyknotic nuclei (Figure 8). The short-arm epitopes for laminin γ2 were prevalent in the glands of the dorsal side (Figures 8f and 8g). The long-arm epitope for laminin γ2 was obvious in the outermost epithelial cell layer (Figure 8h). The immunohistochemical staining patterns for the laminin α3, laminin β3, and keratin type II appeared similar (data not shown).

Laminin γ2 Expression Is in the Leading Edge of a Migratory Epithelial Sheet and Does Not Overlap with Keratin 5

Keratin type II was expressed in both the migrating and proliferating cells (Figures 9a and 9d, green). The keratin 5 was expressed in the basal keratinocytes and not in the migrating cells (Figures 9b and 9d, red). Nuclei were stained blue (Figure 9c). Keratin type II overlapped with keratin 5 (Figure 9d, yellow) in the basal cells, demarcating two epithelial cell populations. Dual labeling confocal immunofluorescent microscopy was performed using antibodies recognizing laminin γ2 (g2 L4) (Figures 10b and 10c, red) and the basal keratinocyte marker, keratin 5 (Figures 10a and 10c, green). Keratin 5 was located in the population of cells positioned underneath the migrating epithelial sheet, primarily the proliferating basal cells and the sebaceous glands (Figures 10a and 10c, green), whereas the laminin γ2 (Figures 10b and 10c red) had a cytoplasmic staining pattern that suggests it is located within endoplasmic reticulum (Figure 10b). The dermis did not express either keratin 5 or laminin γ2. The lack of overlap (yellow) in the merged image (Figure 10c) suggests the laminin γ2 and keratin 5 are not expressed by the same cells. The keratin 5 was in the basal keratinocytes and the laminin γ2 in the migrating epithelial sheet moving across the wound bed. Thus, the laminin γ2 appeared to be in the epithelial cells that have left the cell cycle. Results were identical using other laminin γ2 antibodies (data not shown).

Laminin γ2 mRNA Is Significantly Increased by the 72-h Post-SM Treatment

Since the proform of laminin-332 requires transcription and translation of all three polypeptide chains, we quantitated the mRNA for the three chains for the five time points examined (Figure 11). The α3 and β3 laminin chain mRNAs decreased in the first 24 h postexposure when normalized against näive control samples (Figure 11, upper panel). Their mRNA levels then rise slightly, remaining about 1.4 fold higher through 168 h compared to controls. The laminin γ2 chain mRNA remained steady for the first 24 h after the SM treatment (Figure 11, lower panel) then rose significantly to a maximum level observed at 72

h post-SM treatment (14 fold increase) and remained high through 168 h posttreatment (10 fold increase).

De Novo Synthesis of the Laminin γ2 Chain Is Apparent by the 72-h Post-SM Treatment

Since the mRNA data suggested preferential expression of the laminin γ2 chain, Western blot analysis was performed to confirm that protein translation corresponded to the increase for the laminin γ2 (Figure 12). Both the intact proform of laminin γ2 (150 kDa) and its two processed forms (105 and 80 kDa) increased over time (Figure 12, lanes 7 and 8). The 80-kDa processed form that represents the long arm of the polypeptide appeared to be in higher quantity than the other two forms (Figure 12, lane 8).

DISCUSSION

There is a lack of medical countermeasures against sulfur mustard, a chemical weapon used in a number of conflicts in the past century. Since Sulfur mustard cannot be tested on humans, the mouse ear vesicant model is one of the most useful tools for these studies, but the ideal parameters for the MEVM have yet to be determined. In incisional wounds, there is a somewhat consistent temporal and spatial correlation between inflammatory cell recruitment and morphological events [25]. In contrast, a chemical-induced wound such as sulfur mustard in the MEVM is considerably less predictable and has a wider variety of pathological responses [23,24]. Inflammation occurs within the first 3 days after most adult skin wounds and is accompanied by an influx of neutrophils. Next keratinocyte proliferation and migration occurs with corresponding T cell, monocyte, and macrophage infiltration 3–10 days after the initial wound. Finally, 10–14 days after the initial wound, maturation occurs and mast cells are a prominent cell type. These observations also occur in the vesicant-induced wounds produced in the MEVM; however, the initial skin damage can be quite variable, and the wound repair pathways activation are frequently delayed in comparison to other types of wounds [20]. The proliferation/migration stage as determined by the appearance of keratin 5, a marker of hyperproliferating basal keratinocytes, is frequently 72 h posttreatment in both the MEVM and incisional wound models. Despite the analogous temporal appearance of keratin 5 in the two wound models, the wound site in the MEVM continues to expand for several days, eventually involving the untreated dorsal side. The skin damage to this untreated side often lags behind the treated, side of the ear by about 12–24 h, and the wound repair is not symmetrical; hence, the treated side may start repair processes while the untreated side is at the height of cellular damage and apoptosis. The mechanism for contralateral side damage is unknown, but one working hypothesis is that the SM directly penetrates the cartilage barrier separating the ventral and dorsal ear. In support of this hypothesis is the observation that sometimes a breach in the continuity of the cartilage layer is observed in the 72 h and 168 h post-treated histological sections (data not shown). In the normal time course for incisional wounds, the epithelial repair pathways are generally activated within 1 week postwounding [25]. However, in the MEVM damage frequently increases with time, sometimes producing a second wave of infiltrating cells [20]. These cells appear to exacerbate tissue damage. The large number of infiltrating cells evident in the H&E-stained 72 and 168 h posttreated samples suggest that there might be a delay in the repair process. This occurs despite the histological observation that the

epithelial cell layer thickness is the normal 2–3 cell layers, and the epidermis to dermis attachment appears somewhat intact, observations expected for normal, repaired tissue. Under closer scrutiny, however, it is obvious that many of the epithelial cells contain pyknotic nuclei and in general appeared “unhealthy” when compared to control tissue sections. It is obvious that full tissue repair is not complete by 168 h post-SM exposure in the MEVM and important extracellular proteins such as laminin-332 may not be structurally intact.

Laminin-332 is an essential glycoprotein for skin repair and is composed of three separate polypeptide chains. In injured skin, laminin-332 is purported to function as a keratinocyte migration promoting protein and is found at the leading edge of the migrating keratinocyte sheet that eventually covers the wound bed during normal wound repair [26,27]. Laminin-332 is also required for final attachment of the basal keratinocytes to the dermis in fully repaired tissue. This anchoring function begins by deposition of a very large laminin-332 proform into the extracellular matrix. It is then enzymatically processed to a smaller heterotrimer that directly links the cell membrane of the epidermal basal cells to the underlying basement membrane of the dermis [1,28]. The assembly of the three chains into the proform is a step-wise process. It begins with laminin β3 and laminin γ2 forming a heterodimer followed by the addition of the laminin α3 polypeptide [29]. If transcription and translation are directly proportional to the amount of mRNA made, then the dramatic increase in the levels of the laminin γ2 mRNA compared to the other two chains of laminin-332 at 72 and 168 h suggests the amount of de novo laminin γ2 polypeptide made is far in excess of the other two chains. If this is true then there is more laminin γ2 than can be incorporated into the heterotrimeric proform of laminin-332. The most likely explanation for the excess laminin γ2 chain is that rather than be incorporated into the full-sized laminin-332 protein, the extra laminin γ2 remains as a monomer, as has been reported for some carcinoma cells [17]. Overexpression of laminin γ2 has been reported as a potential marker of invasion of malignant and metastatic cancers, and the possibility remains that in the MEVM it is a marker of epithelial cell migration during wound repair [30]. The work presented here does not directly address the expression of monomeric laminin γ2 and is unable to distinguish between laminin γ2 trapped in the cytoplasm and that secreted extracellularly as a monomer. However, quantitative overexpression of the laminin γ2 mRNA compared to the other two chains of laminin-332 was measured and enhanced protein expression for laminin γ2 was determined indirectly. Like other types of skin injury, it appears that sulfur mustard skin exposure results in homeostatic dysfunction causing endoplasmic reticulum stress response (ESR). The ESR is triggered when any of several perturbations in normal ER function occur (e.g., accumulation of misfolded proteins, lipid imbalances, or excessive ionic changes in the lumen of the endoplasmic reticulum (ER)). In situations of extreme cellular damage (e.g., the MEVM), the ESR is activated to increase the capacity of the ER to fold and process proteins [31]. The confocal microscopy experiments supported the notion that there was accumulation of laminin γ2 in the ER, specifically in the migrating, but not proliferating cells. This observation is consistent with a recent report that laminin-332 is found in migrating transformed epithelial cells that have left the cell cycle, but not in proliferating cells [32,33]. Western blot analysis showed that for the 72 and 168 h time points, the laminin γ2 protein directly increased in proportion to time after exposure for

both the unprocessed, full length, proform of laminin γ2 (upper band; Figure 12, lanes 7 and 8) and its smaller, 105 kDa processed form γ2 (middle band; Figure 12, lanes 7 and 8). There appeared to be a preferential increase of the completely processed long arm γ2 (80 kDa, lower band; Figure 12, lanes 7 and 8), suggesting the short arm was clipped off. This observation supported the immunohistochemistry data where the signal for the long-arm antibody was very strong in the 168 posttreated samples on the dorsal side (Figure 8h). Whether the signal represents the unprocessed or processed form cannot be determined from this figure. What is clear is that the signal was much stronger for the long arm than for the short-arm epitopes (Figures 3f and 3g), indicating the long arm is present in the matrix, while the short arm is more soluble in the epidermis. The short arm is, however, clearly present in the glands. All the evidence to date indicates that processing of all three laminin-332 chains occurs by enzymes in the extracellular matrix and not in the cytoplasm. Since the Western blot data indicates there is processing of the laminin γ2 chain to smaller sizes, our interpretation is that there is a significant amount of processed laminin γ2 that is available as a monomer in the ECM in response to wounding [34]. The processing and release of the short arm from the monomer would allow it to participate in cell migration as part of the normal wound repair process analogous to the processed laminin γ2 migration enhancing properties in transformed epithelial cells [34,35]. Although the precise mechanism of action for migration promotion by monomeric laminin γ2 is still unknown, one theory suggests that the proteolytic processing of laminin γ2 and subsequent release of an EGF-like domain (g2 LEb3–5) stimulates cell migration by binding to the epidermal growth factor receptor [36]. This domain would be present in our model, but clipped off from the long arm and not recognized by the antibody used for the Western blot analysis (the antibody does, however, recognize the abundant 80 kDa long arm left behind, and the presumption is that the released short arm is equally abundant). Taken together, all the data, support the dual functions attributed to laminin-332: those of cell adhesion and cell migration. First, there appears to be expression of all three chains of laminin-332 to allow the proform to be secreted into the ECM where it can be processed to the cell adhesion form. Second, the severely damaged cells demonstrate an ERS response, but still secrete abundant, monomeric, processed, laminin γ2, which are available for enhancing cell migration over the wound bed. Although the data presented here have not definitively proved a cause and effect, further studies are planned to confirm that monomeric laminin γ2 protein is present in the extra-cellular matrix in the MEVM.

ACKNOWLEDGMENTS

We thank to Rita Hahn for technical support, Linda Everett for editorial work and figure preparation, and Dr John Graham, USAMRICD, Aberdeen Proving Ground, MD, for his excellent suggestions regarding this research.

Contract Grant Sponsor: NIH CounterACT Program through the National Institute of Arthritis and Musculoskeletal and Skin Diseases.

Contract Grant Number: U54AR055073.

Contract Grant Sponsor: NIEHS sponsored UMDNJ Center for Environmental Exposures and Disease.

Contract Grant Number: P30ES005022.

Contract Grant Sponsor: NIH/NIEHS-funded Training in Environmental Toxicology.

Contract Grant Number: ES004738.

Contract Grant Sponsor: NIH/NEI-funded Expression of Specialized Collagens in Cornea.

Contract Grant Number: EY09056.

Its contents are solely the responsibility of the authors and do not necessarily represent the official views of the funding agencies.

REFERENCES

1. Rousselle P, Lunstrum GP, Keene DR, Burgeson RE. Kalinin: an epithelium-specific basement membrane adhesion molecule that is a component of anchoring filaments. J Cell Biol. 1991; 114(3): 567–576. [PubMed: 1860885]
2. Miyazaki K. 5 (laminin-332): Unique biological activity and role in tumor growth and invasion. Cancer Sci. 2006; 97(2):91–98. [PubMed: 16441418]
3. Marinkovich MP. Tumour microenvironment: laminin 332 in squamous-cell carcinoma. Nat Rev Cancer. 2007; 7(5):370–380. [PubMed: 17457303]
4. Niessen CM, Hogervorst F, Jaspars LH, de Melker AA, Delwel GO, Hulsman EH, Kuikman I, Sonnenberg A. The α6β4 integrin is a receptor for both laminin and kalinin. Exp Cell Res. 1994; 211(2):360–367. [PubMed: 8143784]
5. Sigle RO, Gil SG, Bhattacharya M, Ryan MC, Yang TM, Brown TA, Boutaud A, Miyashita Y, Olerud J, Carter WG. Globular domains 4/5 of the laminin α3 chain mediate deposition of precursor laminin 5. J Cell Sci. 2004; 117(Pt 19):4481–4494. [PubMed: 15316072]
6. Rousselle P, Keene DR, Ruggiero F, Champliaud MF, Rest M, Burgeson RE. Laminin 5 binds the NC-1 domain of type VII collagen. J Cell Biol. 1997; 138(3):719–728. [PubMed: 9245798]
7. Chen M, Marinkovich MP, Jones JC, O'Toole EA, Li YY, Woodley DT. NC1 domain of type VII collagen binds to the β3 chain of laminin 5 via a unique subdomain within the fibronectin-like repeats. J Invest Dermatol. 1999; 112(2):177–183. [PubMed: 9989793]
8. Marinkovich MP, Lunstrum GP, Burgeson RE. The anchoring filament protein kalinin is synthesized and secreted as a high molecular weight precursor. J Biol Chem. 1992; 267(25):17900–17906. [PubMed: 1517226]
9. Nakashima Y, Kariya Y, Yasuda C, Miyazaki K. Regulation of cell adhesion and type VII collagen binding by the β3 chain short arm of laminin-5: effect of its proteolytic cleavage. J Biochem. 2005; 138(5):539–552. [PubMed: 16272566]
10. Hintermann E, Quaranta V. Epithelial cell motility on laminin-5: regulation by matrix assembly, proteolysis, integrins and erbB receptors. Matrix Biol. 2004; 23(2):75–85. [PubMed: 15246107]
11. Giannelli G, Falk-Marzillier J, Schiraldi O, Stetler-Stevenson WG, Quaranta V. Induction of cell migration by matrix metalloprotease-2 cleavage of laminin-5. Science. 1997; 277(5323):225–228. [PubMed: 9211848]
12. Miyazaki K, Kikkawa Y, Nakamura A, Yasumitsu H, Umeda M. A large cell-adhesive scatter factor secreted by human gastric carcinoma cells. Proc Natl Acad Sci USA. 1993; 90(24):11767–11771. [PubMed: 8265624]
13. Bachy S, Letourneur F, Rousselle P. Syndecan-1 interaction with the LG4/5 domain in laminin-332 is essential for keratinocyte migration. J Cell Physiol. 2008; 214(1):238–249. [PubMed: 17579341]
14. Momota Y, Suzuki N, Kasuya Y, Kobayashi T, Mizoguchi M, Yokoyama F, Nomizu M, Shinkai H, Iwasaki T, Utani A. Laminin α3 LG4 module induces keratinocyte migration: involvement of matrix metalloproteinase-9. J Recept Signal Transduct Res. 2005; 25(1):1–17. [PubMed: 15960391]
15. Utani A, Momota Y, Endo H, Kasuya Y, Beck K, Suzuki N, Nomizu M, Shinkai H. Laminin α3 LG4 module induces matrix metalloproteinase-1 through mitogen-activated protein kinase signaling. J Biol Chem. 2003; 278(36):34483–34490. [PubMed: 12826666]

16. Ogawa T, Tsubota Y, Maeda M, Kariya Y, Miyazaki K. Regulation of biological activity of laminin-5 by proteolytic processing of γ2 chain. J Cell Biochem. 2004; 92(4):701–714. [PubMed: 15211568]
17. Koshikawa N, Moriyama K, Takamura H, Mizushima H, Nagashima Y, Yanoma S, Miyazaki K. Overexpression of laminin γ2 chain monomer in invading gastric carcinoma cells. Cancer Res. 1999; 59(21):5596–5601. [PubMed: 10554040]
18. Goldfinger LE, Hopkinson SB, deHart GW, Collawn S, Couchman JR, Jones JC. The α3 laminin subunit, α6β4 and α3β1 integrin coordinately regulate wound healing in cultured epithelial cells and in the skin. J Cell Sci. 1999; 112(Pt. 16):2615–2629. [PubMed: 10413670]
19. Lampe PD, Nguyen BP, Gil S, Usui M, Olerud J, Takada Y, Carter WG. Cellular interaction of integrin α3β1 with laminin 5 promotes gap junctional communication. J Cell Biol. 1998; 143(6): 1735–1747. [PubMed: 9852164]
20. Casillas RP, Kiser RC, Truxall JA, Singer AW, Shumaker SM, Niemuth NA, Ricketts KM, Mitcheltree LW, Castrejon LR, Blank JA. Therapeutic approaches to dermatotoxicity by sulfur mustard, I. Modulation of sulfur mustard-induced cutaneous injury in the mouse ear vesicant model. J Appl Toxicol. 2000; 20(Suppl. 1):S145–S151. [PubMed: 11428628]
21. Shakarjian MP, Bhatt P, Gordon MK, Chang YC, Casbohm SL, Rudge TL, Kiser RC, Sabourin CL, Casillas RP, Ohman-Strickland P, Riley DJ, Gerecke DR. Preferential expression of matrix metalloproteinase-9 in mouse skin after sulfur mustard exposure. J Appl Toxicol. 2006; 26(3): 239–246. [PubMed: 16489579]
22. Sasaki T, Gohring W, Mann K, Brakebusch C, Yamada Y, Fassler R, Timpl R. Short arm region of laminin-5 γ2 chain: structure, mechanism of processing and binding to heparin and proteins. J Mol Biol. 2001; 314(4):751–763. [PubMed: 11733994]
23. Monteiro-Riviere NA, Inman AO, Babin MC, Casillas RP. Immunohistochemical characterization of the basement membrane epitopes in bis(2-chloroethyl) sulfide-induced toxicity in mouse ear skin. J Appl Toxicol. 1999; 19(5):313–328. [PubMed: 10513676]
24. Smith KJ, Casillas R, Graham J, Skelton HG, Stemler F, Hackley BE Jr. Histopathologic features seen with different animal models following cutaneous sulfur mustard exposure. J Dermatol Sci. 1997; 14(2):126–135. [PubMed: 9039976]
25. Stramer BM, Mori R, Martin P. The inflammation-fibrosis link? A Jekyll and Hyde role for blood cells during wound repair. J Invest Dermatol. 2007; 127(5):1009–1017. [PubMed: 17435786]
26. Nguyen BP, Gil SG, Carter WG. Deposition of laminin 5 by keratinocytes regulates integrin adhesion and signaling. J Biol Chem. 2000; 275(41):31896–31907. [PubMed: 10926936]
27. Nguyen BP, Ryan MC, Gil SG, Carter WG. Deposition of laminin 5 in epidermal wounds regulates integrin signaling and adhesion. Curr Opin Cell Biol. 2000; 12(5):554–562. [PubMed: 10978889]
28. Carter WG, Ryan MC, Gahr PJ. Epiligrin, a new cell adhesion ligand for integrin α3β1 in epithelial basement membranes. Cell. 1991; 65(4):599–610. [PubMed: 2032285]
29. Matsui C, Wang CK, Nelson CF, Bauer EA, Hoeffler WK. The assembly of laminin-5 subunits. J Biol Chem. 1995; 270(40):23496–23503. [PubMed: 7559513]
30. Kagesato Y, Mizushima H, Koshikawa N, Kitamura H, Hayashi H, Ogawa N, Tsukuda M, Miyazaki K. Sole expression of laminin γ2 chain in invading tumor cells and its association with stromal fibrosis in lung adenocarcinomas. Jpn J Cancer Res. 2001; 92(2):184–192. [PubMed: 11223548]
31. Boyce M, Yuan J. Cellular response to endoplasmic reticulum stress: a matter of life or death. Cell Death Differ. 2006; 13(3):363–373. [PubMed: 16397583]
32. Natarajan E, Omobono JD II, Guo Z, Hopkinson S, Lazar AJ, Brenn T, Jones JC, Rheinwald JG. A keratinocyte hypermotility/growth-arrest response involving laminin 5 and p16INK4A activated in wound healing and senescence. Am J Pathol. 2006; 168(6):1821–1837. [PubMed: 16723698]
33. Svensson Mansson S, Reis-Filho J, Landberg G. Transcriptional upregulation and unmethylation of the promoter region of p16 in invasive basal cell carcinoma cells and partial co-localization with the γ2 chain of laminin-332. J Pathol. 2007; 212(1):102–111. [PubMed: 17370299]
34. Natarajan E, Omobono JD II, Jones JC, Rheinwald JG. Co-expression of p16INK4A and laminin 5 by keratinocytes: a wound-healing response coupling hypermotility with growth arrest that goes awry during epithelial neoplastic progression. J Investig Dermatol Symp Proc. 2005; 10(2):72–85.

35. Natarajan E, Saeb M, Crum CP, Woo SB, McKee PH, Rheinwald JG. Co-expression of p16(INK4A) and laminin 5 γ2 by microinvasive and superficial squamous cell carcinomas in vivo and by migrating wound and senescent keratinocytes in culture. Am J Pathol. 2003; 163(2):477–491. [PubMed: 12875969]

36. Schenk S, Hintermann E, Bilban M, Koshikawa N, Hojilla C, Khokha R, Quaranta V. Binding to EGF receptor of a laminin-5 EGF-like fragment liberated during MMP-dependent mammary gland involution. J Cell Biol. 2003; 161(1):197–209. [PubMed: 12695504]

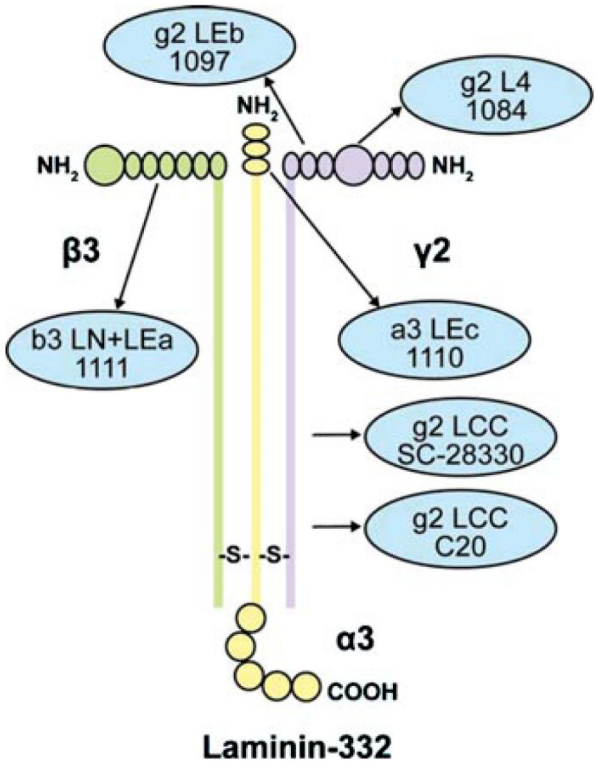

FIGURE 1.

Schematic diagram of the intact laminin-332 protein indicating the domains recognized by antibodies used for analysis. The antibodies directed toward specific protein domains are indicated by arrows and blue circles.

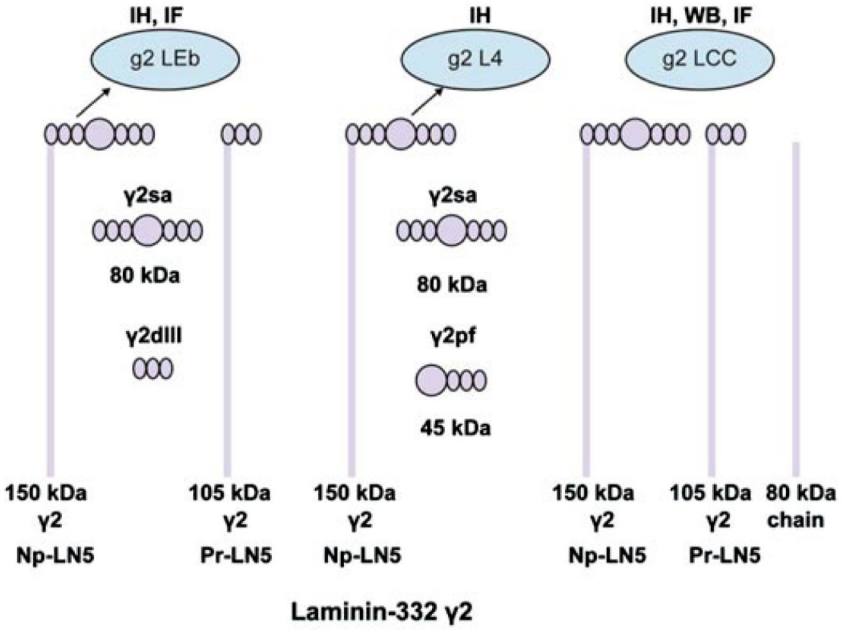

FIGURE 2.

Laminin-332 can be processed into many possible fragments. The processed forms of laminin-332 γ2 recognized by the various antibody epitopes used in the studies are indicated. Antibody g2 LEb recognizes epidermal growth factor-like domain 2 found in short-arm domain III. Antibody g2 L4 recognizes short-arm globular domain IV. Antibody g2 LCC recognizes the long-arm domain I/II. Abbreviations: IH, immunohistochemistry: IF, immunofluorescence: WB, Western blot.

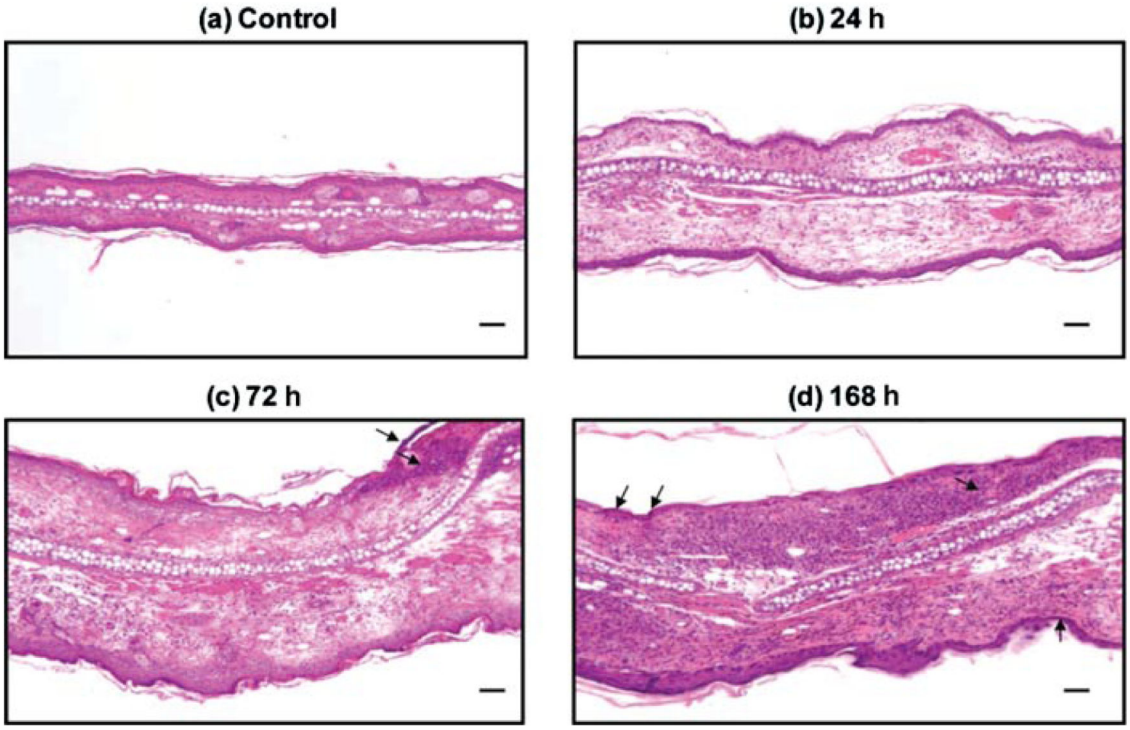

FIGURE 3.

Hemotoxylin and eosin staining of mouse ear paraffin sections. The ventral (inner) ear is the upper surface, and the dorsal (outer, untreated side) is the lower surface. Panel (a): Untreated control showing the dense tissue morphology. The central white area is cartilage separating the ventral and dorsal sides. Both sides have sebaceous glands seen very clearly in the control (a) as light pink circles in the dermis. The dorsal side also typically has striated muscle adjacent to the cartilage, which is not present in the ventral side. (b) 24 h, (c) 72 h, and (d) 168 h, are ears from animals treated with SM. All SM-treated ears demonstrate edema as indicated by the increased white space and much larger distance separating the ventral and dorsal sides. Inflammatory cell infiltration increases over time (purple dots, which are maximum at 168 h posttreatment) as does necrosis (c, d, arrows). Bar=100 μm.

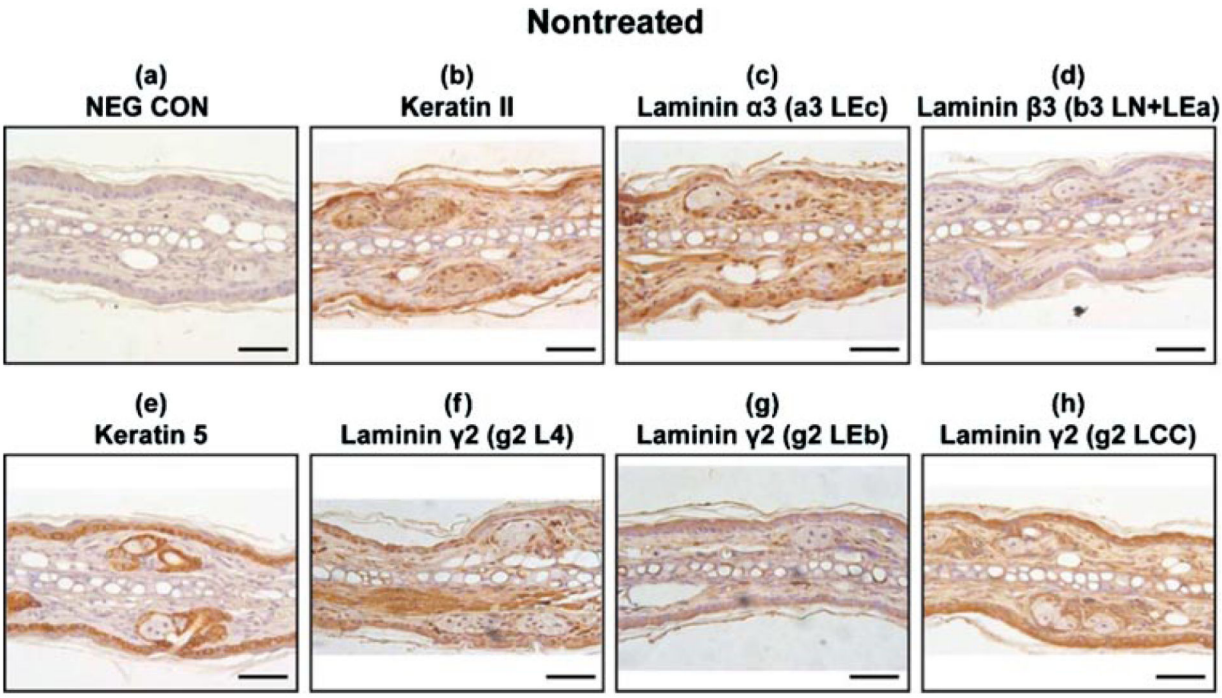

FIGURE 4.

Immunohistochemistry of nontreated control mouse ear paraffin sections using various markers with brown indicating the positive staining areas: (a) negative control; (b) keratin type II; (c) laminin α3 domain a3 LEc (Figure 1); (d) laminin β3 domain b3 LN + LEa (Figure 1); (e) keratin 5; (f) laminin γ2 domain g2 L4 (Figures 1 and 2); (g) laminin γ2 domain g2 LEb (Figures 1 and 2); (h) laminin γ2 domain g2 LCC (Figures 1 and 2). Bar=100 μm.

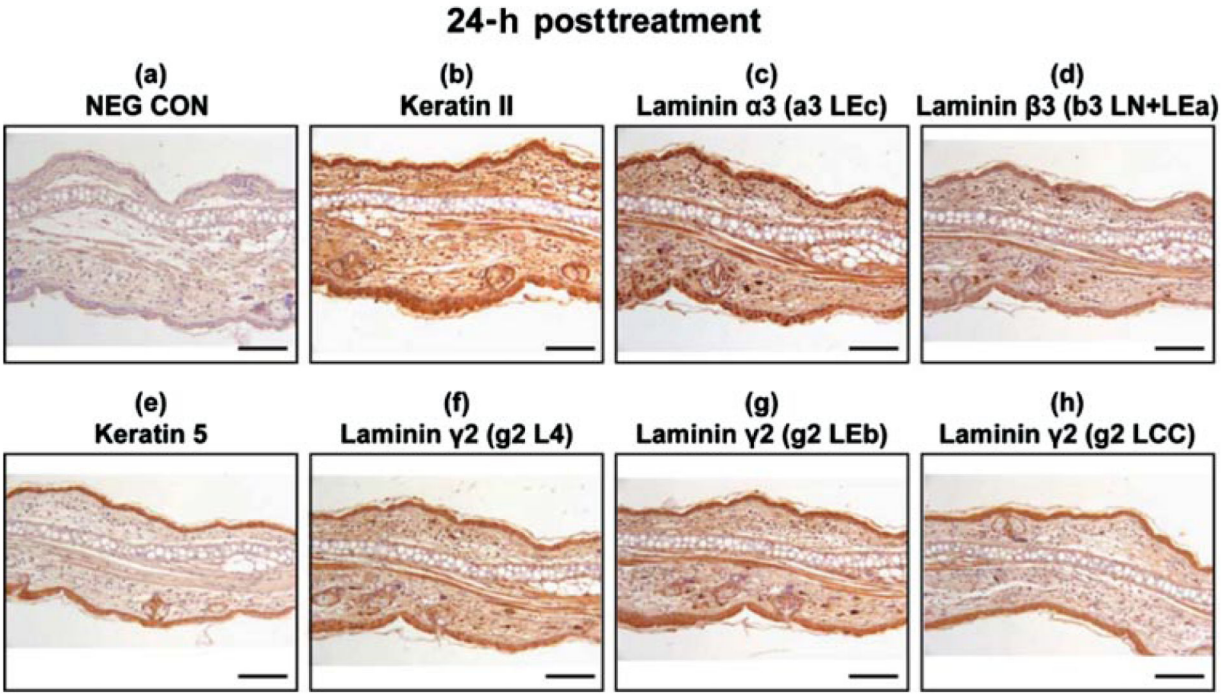

FIGURE 5.

Immunohistochemistry of mouse ear paraffin sections 24 h post-SM treatment using various markers with brown indicating the positive staining areas: (a) negative control; (b) keratin type II; (c) laminin α3 domain a3 LEc; (d) laminin β3 domain b3 LN + LEa; (e) keratin 5; (f) laminin γ2 domain g2 L4; (g) laminin γ2 domain g2 LEb; (h) laminin γ2 domain g2 LCC. Bar=100 μm.

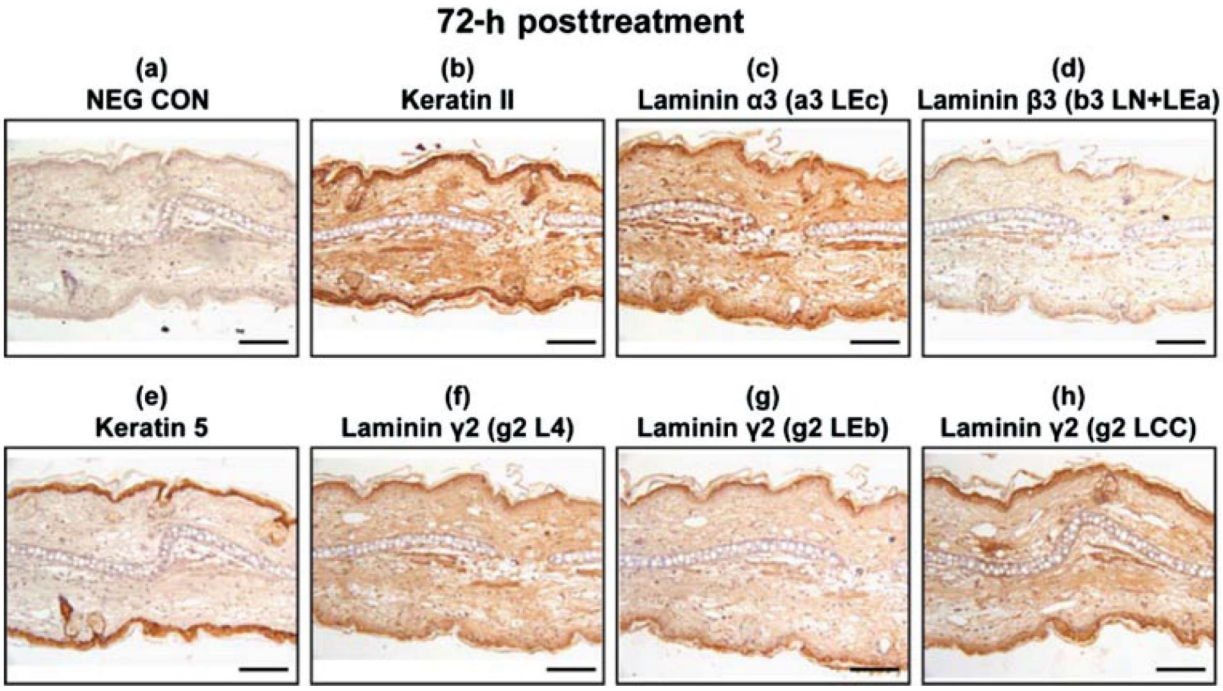

FIGURE 6.

Immunohistochemistry of mouse ear paraffin sections 72 h post-SM treatment using various markers with brown indicating the positive staining areas: (a) negative control; (b) keratin type II; (c) laminin α3 domain a3 LEc; (d) laminin β3 domain b3 LN + LEa; (e) keratin 5; (f) laminin γ2 domain g2 L4; (g) laminin γ2 domain g2 LEb; (h) laminin γ2 domain g2 LCC. Bar=100 μm.

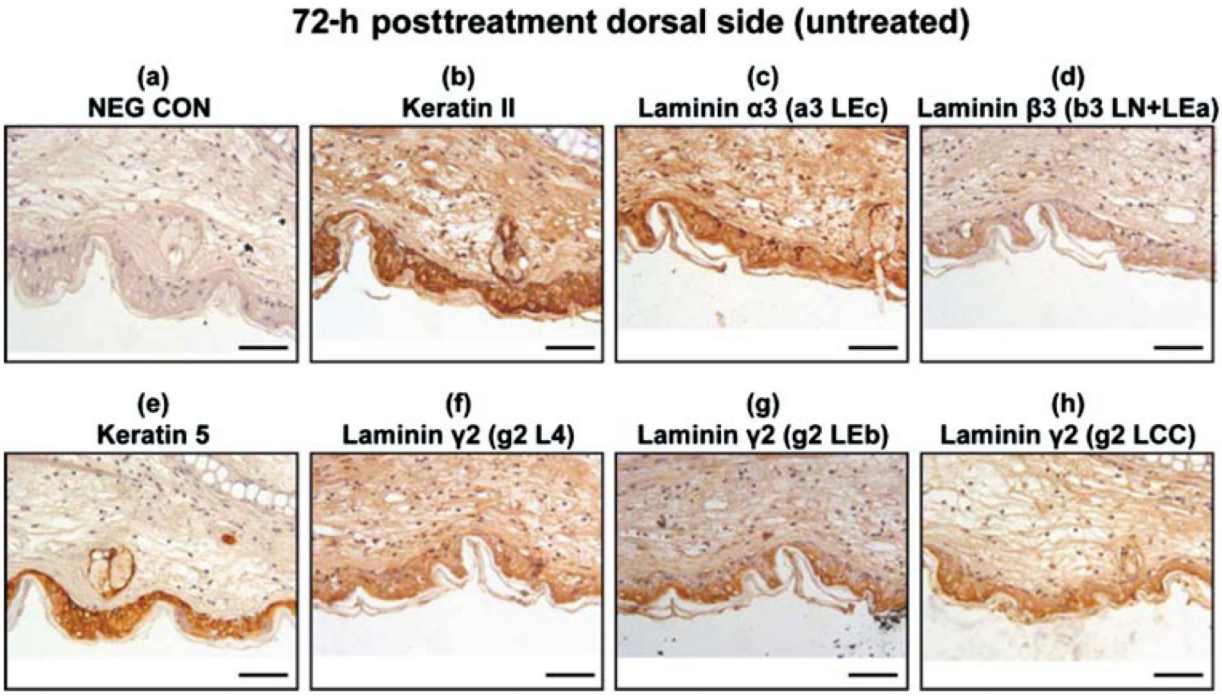

FIGURE 7.

Immunohistochemistry of dorsal (untreated side) mouse ear paraffin sections 72 h post-SM treatment using various markers: (a) negative control; (b) keratin type II; (c) laminin α3 domain a3 LEc; (d) laminin β3 domain b3 LN + LEa; 7(e) keratin 5; (f) laminin γ2 domain g2 L4; (g) laminin γ2 domain g2 LEb; (h) laminin γ2 domain g2 LCC. Bar=100 μm.

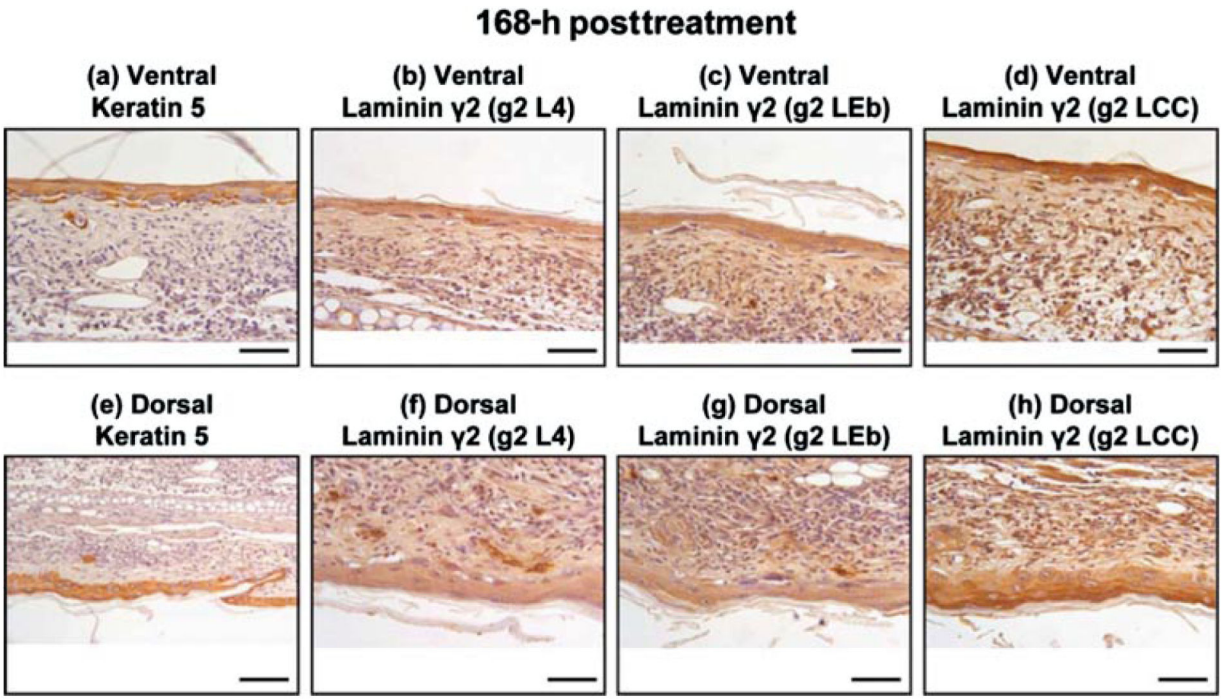

FIGURE 8.

Immunohistochemistry of mouse ear paraffin sections 168 h post-SM treatment using various markers: Upper panels are the ventral, treated side: from left to right: (a) keratin 5; (b) laminin γ2 domain g2 L4; (c) laminin γ2 domain g2 LEb; (d) laminin γ2 domain g2 LCC. Lower panels are the dorsal, untreated side: from left to right: (e) keratin 5; (f) laminin γ2 domain g2 L4; (g) laminin γ2 domain g2 LEb; (h) laminin γ2 domain g2 LCC. Bar = 100 μm.

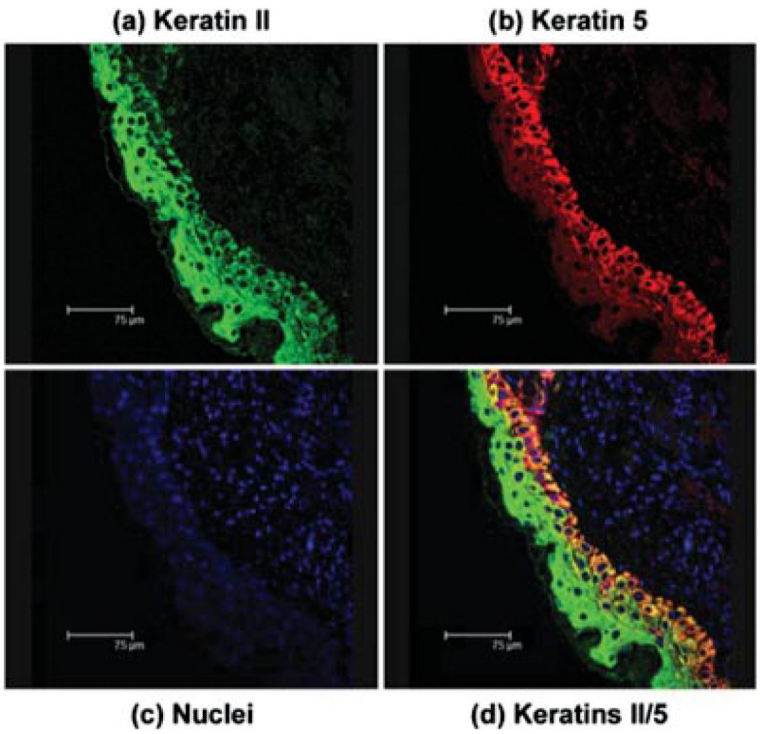

FIGURE 9.

Projected confocal micrograph of keratin type II and keratin 5 in 72 h SM posttreated mouse ear paraffin section. (a) keratin type II (green) was distributed throughout the epithelium; (b) keratin 5 (red) was restricted to the basal epithelial cell layer; (c) nuclei (blue) show the tissue section included the epidermis and dermis; (d) merged image (green/red/yellow) demonstrates the overlap of keratin 5 (green) and keratin type II (red) in the epithelium with some yellow in the basal cells and no staining in the dermis. Bar = 75 μm.

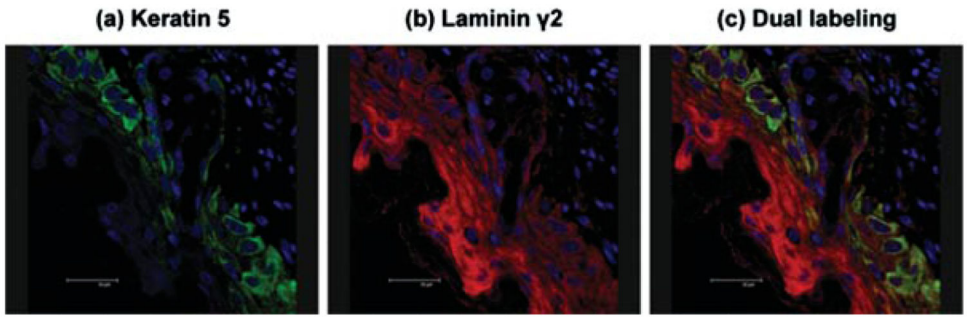

FIGURE 10.

Projected confocal micrograph of keratin 5 and laminin γ2 in 72 h SM posttreated mouse ear section. (a) keratin 5 (green) labeled the basal epithelial cell population and the gland cells; (b) laminin γ2 (red) was expressed in the suprabasal cells in a cytoplasmic pattern; (c) merged image of keratin 5 (green) and laminin γ2 (red) demonstrated that there was very little overlap in the two proteins. Bar=30 μm.

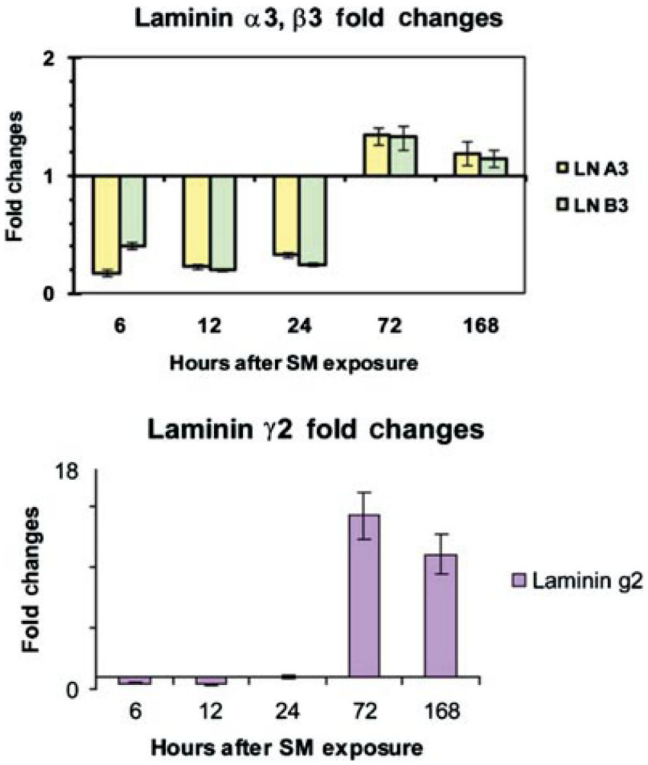

FIGURE 11.

RT-PCR determined fold changes of mRNA for individual polypeptide chains of laminin-332 after the SM treatment in mouse ears. Upper panel represents laminin α3 and laminin β3 mRNA fold changes 6, 12, 24, 72, and 168 h post-SM treatment. Bottom panel represents laminin γ2 mRNA fold changes 6, 12, 24, 72, and 168 h post-SM treatment.

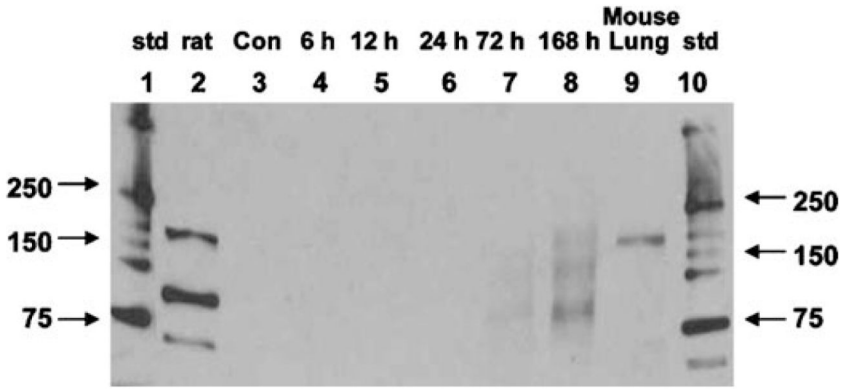

FIGURE 12.

Time course Western blot analysis of laminin γ2 in SM-treated mouse ears. Lanes are as follows: (1) molecular weight standards; (2) control rat LN-332; (3) 168 h untreated mouse LN-332; (4) 6 h SM-treated mouse LN-332; (5) 12 h SM-treated mouse LN-332; (6) 24 h SM-treated mouse LN-332; (7) 72 h SM-treated mouse LN-332; (8) 168 h SM-treated mouse LN-332; (9) mouse lung extract